

Electrical characterization of single cells using polysilicon wire ion sensor in an isolation window

You-Lin Wu · Po-Yen Hsu · Chung-Ping Hsu ·
Chih-Cheng Wang · Li-Wen Lee · Jing-Jenn Lin

Published online: 22 June 2011
© Springer Science+Business Media, LLC 2011

Abstract A polysilicon wire (PSW) sensor can detect the H^+ ion density (pH value) of the medium coated on its surface, and different cells produce different extracellular acidification and hence different H^+ ion densities. Based on this, we used a PSW sensor in combination with a mold-cast polydimethylsiloxane (PDMS) isolation window to detect the adhesion, apoptosis and extracellular acidification of single normal cells and single cancer cells. Single living human normal cells WI38, MRC5, and BEAS-2B as well as non-small-cell lung cancer (NSCLC) cells A549, H1299, and CH27 were cultivated separately inside the isolation window. The current flowing through the PSW channel was measured. From the PSW channel current change as a function of time, we determined the cell adhesion time by observing the time required for the current change to saturate, since a stable extracellular ion density was established after the cells were completely adhered to

the PSW surface. The apoptosis of cells can also be determined when the channel current change drops to zero. We found that all the NSCLC cells had a higher channel current change and hence a lower pH value than the normal cells anytime after they were seeded. The corresponding average pH values were 5.86 for A549, 6.00 for H1299, 6.20 for CH27, 6.90 for BEAS-2B, 6.96 for MRC5, and 7.02 for WI38, respectively, after the cells were completely adhered to the PSW surface. Our results show that NSCLC cells have a stronger cell-substrate adhesion and a higher extracellular acidification rate than normal cells.

Keywords Single cell detection · Extracellular acidification · Polysilicon wire

1 Introduction

The characterization of cells with a large population such as in traditional biochemical analysis, using for example radioactive detection, immunoblotting technique, or immunofluorescence analysis, often overlooks the information regarding the heterogeneity of the individual cell (Ferrell and Machleder 1998) (Teruel and Meyer 2002) and likely results in some misleading conclusions. Therefore, single cell analysis has become an essential requirement for a more accurate interpretation of cell behavior. Many techniques such as capillary electrophoresis (CE) (Krylov and Docichi 2000) (Chen and Lillard 2001) (Wood et al. 2004) and flow cytometry (Davey and Kell 1996) (Vermes et al. 2000) have been developed for single cell analysis. In these studies, cells labeled with fluorescence conjugates are injected into a capillary tube (or a microfluidic channel) so that one single cell at a time flows through the capillary tube (or a microfluidic channel) and is being detected. With

Y.-L. Wu (✉) · P.-Y. Hsu
Department of Electrical Engineering,
National Chi Nan University,
Puli, Nantou 54561, Taiwan R.O.C.
e-mail: ylwu@ncnu.edu.tw

C.-P. Hsu · L.-W. Lee
Division of Thoracic Surgery, Department of Surgery,
Taichung Veterans General Hospital,
Taichung 40705, Taiwan R.O.C.

C.-C. Wang
Graduate Institute of Biomedicine and Biomedical Technology,
National Chi Nan University,
Puli, Nantou 54561, Taiwan R.O.C.

J.-J. Lin
Department of Applied Materials and Optoelectronic Engineering,
National Chi Nan University,
Puli, Nantou 54561, Taiwan R.O.C.

these techniques, however, adding fluorescent conjugates may alter the original cellular functions of the cells (Fujita and Smith 2008) making real-time monitoring of different biophysical properties of a single cell difficult to achieve because different fluorescent conjugates have to be added simultaneously, and because multicolor fluorescence microscopy has to be used (Sims and Allbritton, 2007).

The advent of nanofabrication has made it possible to propose nanoparticles, carbon nanotubes and nanowires for biomedical research and analysis (Roco 2003) (Andersson and van den Berg 2004) (Patolsky et al. 2006) (Karni et al. 2009) (Baumann et al. 1999) (Pui et al. 2009). Silicon nanowire (SiNW) field-effect transistors have been used to detect the neuronal signal of a single neuron cell and a single muscle cell (Patolsky et al. 2006) (Karni et al. 2009). The high sensitivity of SiNW field-effect transistors is very attractive, but the alignment difficulty and the low yield of fabrication make that the SiNW is still not very popular for cell detection. At the same time, detecting cells or rat cardiomyocytes confined in a sensing area has also been proposed in previous reports (Baumann et al. 1999) (Pui et al. 2009). Single-cell detection in a confined sensitive area has also been achieved by using sensors such as the microelectrode array (Chen et al. 2003) (Gray et al. 2004) (Revzin et al. 2004), the open-gate field-effect transistor (Baumann et al. 1999) (Schäfer et al. 2009) (Sommerhage et al. 2010) arrays, and SiNW transistor arrays (Patolsky et al. 2006) (Karni et al. 2009). In this work, we used mold-cast PDMS for the confined sensitive area (isolation window). Prior to fabricating the isolation window, a γ -APTES layer with an area about the same size of a cell was coated onto the PSW sensor surface inside the isolation window. This fabrication process allows a single cell to be cultivated with ease in the isolation window. In contrast to the assays using a confined sensitive area for single cell detection as mentioned earlier, our approach does not need a reference electrode, patch pipette, or patch-clamp amplifier. In addition, in our case no cytoskeletal filaments extend outside the confined sensitive area and the single cell is completely isolated inside the PDMS isolation window, thereby allowing the electrical measurement of the PSW to reflect the microenvironment properties of the single cell.

The advantage of using PSW rather than SiNW is that PSW is much less-expensive and is readily fabricated by conventional semiconductor fabrication methods without losing much sensitivity (Mishra et al. 2008) (Hsiao et al. 2009) (Hsu et al. 2009) (Wu et al. 2010) (Wu et al. 2011). It is known that the extracellular metabolic microenvironment is highly related to cell properties such as cell migration and invasion (Gillies et al. 1994) (McCoy et al. 1995) (Raghunand et al. 1999) (Gatenby and Gillies 2004)

(Cardone et al. 2005). It has been proven that, compared to normal tissue, tumors require a high level of glucose so as to consistently acidify their environment in order to support the metabolism, resulting in a lower extracellular pH value. Since a PSW sensor has been proven to be able to detect the H^+ ion density (pH value) of the medium coated on the PSW surface (Hsu et al. 2009) (Wu et al. 2011) and different cells produce different extracellular acidification and hence different H^+ ion densities (Baumann et al. 1999) (Schäfer et al. 2009) (Sommerhage et al. 2010), it is therefore expected that any change in the extracellular microenvironment of the single cell confined in the isolation window residing on the PSW will alter the surface-charge state of the PSW and can therefore be detected by the change in the current flowing through the PSW channel. In this paper, we report for the first time the differences in extracellular cell property between normal cells and cancer cells by using a PSW in combination with an isolation window.

2 Materials and methods

2.1 PSW sensor

P-type (100) silicon wafer was used as the substrate in this work. After the standard RCA clean (Kern and Puotinen 1970), a 12 nm-thick thermal oxide was grown at 900°C. A phosphorous-doped polysilicon layer with a thickness of 80 nm and a sheet resistance of 40–50 Ω/\square was then deposited onto the oxide layer at 620°C by vertical furnace. An e-beam writer was used to define the pattern of the PSW. After development, the poly-Si wire was created by reactive-ion-etching. The line width and length of the PSW are 200 nm and 3 μm , respectively. With the help of an optical microscope, a 1 μL 3-aminopropyltriethoxysilane (γ -APTES) ethanol solution (1%) was dropped onto the PSW surface by micropipette, followed by a 5 min curing process at 120°C to improve the adhesion of living cells to the PSW surface (Lee et al. 2005). The γ -APTES layer covers mainly the central area of the PSW surface measuring about 0.132 mm^2 , which is about the size of a single cell and ensures single cell adhesion. The area of the γ -APTES layer was estimated from the solution volume loaded into the micropipette and the after-coating thickness measured by atomic force microscope.

First, a square mold, measuring 200 $\mu\text{m} \times 200 \mu\text{m} \times 400 \mu\text{m}$ used to fabricate the isolation window was defined and developed by standard photolithographic process using the negative photoresist SU-8-2,150 (Microchem, U.S.A.). After curing at 200°C for 30 min, a PDMS solution (Sylgard 184, Dow Corning) mixed with Sylgard 184

curing agent in a 10:1 ratio was then poured into the square photoresist mold. This was then followed by a 65°C, 12 h curing process in vacuum. After being peeled off from the mold, the PDMS isolation window was subjected to UV irradiation (wavelength $\lambda = 365$ nm) for 40 min to convert it from hydrophobic to hydrophilic (Schnyder et al. 2003) (Berdichevsky et al. 2004). Then, with the help of an optical microscope, the PDMS isolation window was placed and adhered onto the γ -APTES coated PSW surface by using a tweezer. Figure 1 illustrates the installation process of the PDMS isolation window onto the surface of the PSW sensor. The fabrication process of the PDMS isolation window is illustrated in Fig. 1(a). Figure 2(a) shows a top-view, by scanning electron microscopy (SEM) of the PSW sensor, and Fig. 2(b) shows the top-view by optical microscopy of the PSW sensor integrated with an isolation window. After being placed into an autoclave sterilizer for sterilization at 110°C for 90 min in vacuum, the PSW sensor with an isolation window was then ready for cell culture.

2.2 Cell culture

Before cultivating the cells on the PSW surface, different cell lines were cultured in their respective culture medium in petri dishes. In other words, the human lung fibroblast cell WI38 was in a 5 c.c. Eagle's minimum essential medium (MEM) containing 10% fetal bovine serum (FBS) supplemented with 10 mL/L penicillin/streptomycin and 10

mL/L L-glutamine (Life Technologies, Inc., Frederick, MD). The human lung fibroblast cell MRC5 was in a 5 c.c. Eagle's Basal Medium (BME) containing 10% FBS supplemented with non-essential amino acid with 2 mM L-glutamine (Life Technologies, Inc., Frederick, MD). The

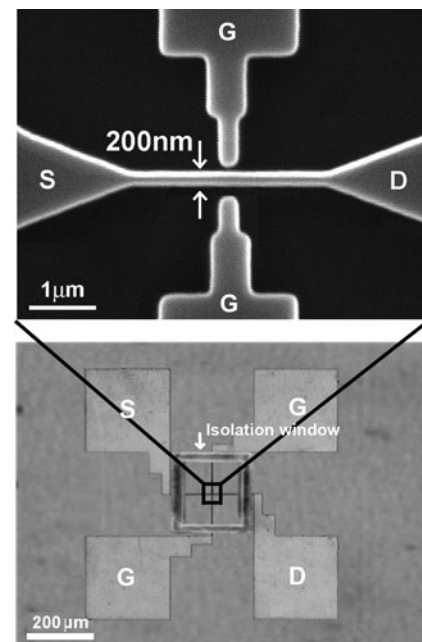


Fig. 2 (a) Top-view by SEM of the PSW sensor, and (b) top-view by optical microscopy of the PSW sensor integrated with an isolation window

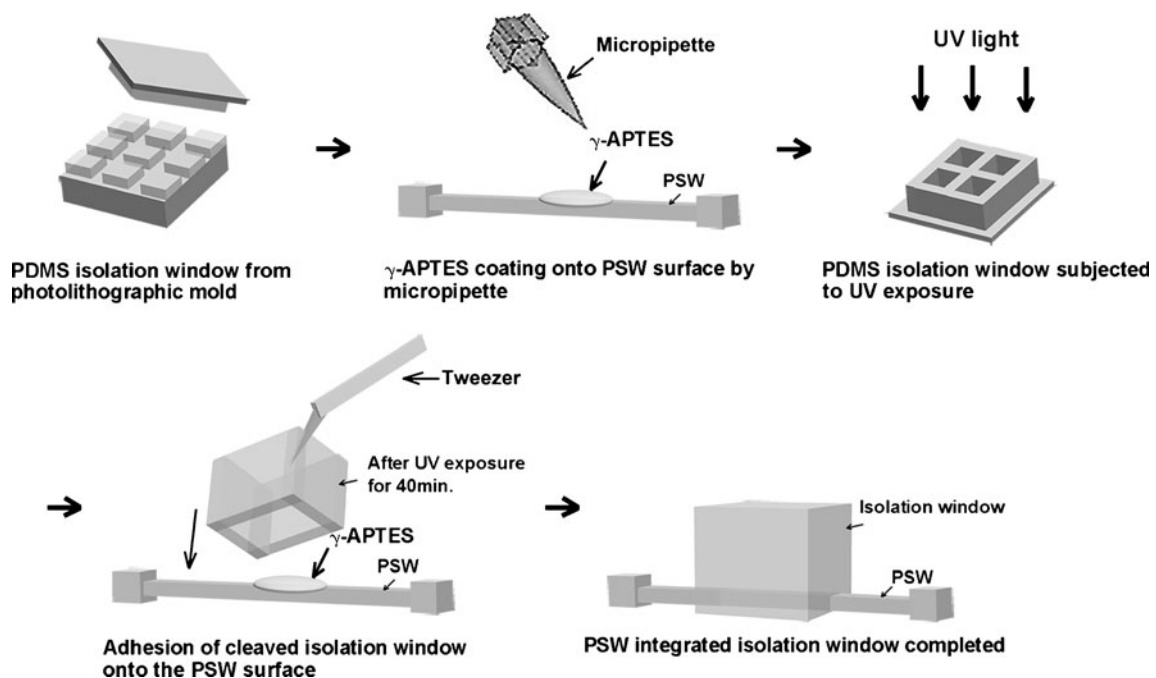


Fig. 1 A schematic of the fabrication process for the PDMS isolation window

human bronchial epithelium cell Beas-2B (obtained from the American Type Culture Collection, Manassas, VA) was in a 5 c.c. RPMI 1,640 medium (Invitrogen; U.S.A.). The human lung adenocarcinoma cancer cells A549 and H1299 (obtained from the American Type Culture Collection, Manassas, VA) were in a 5 c.c. Dulbecco's modified Eagle's medium (DMEM) containing 10% FBS supplemented with penicillin (50 units/mL) and streptomycin (50 $\mu\text{g/mL}$), and the human lung squamous-cell carcinoma CH27 was in a 5 c.c. RPMI 1,640 medium containing 10% FBS supplemented with 2mM L-glutamine/antibiotic-antimycotic and 2g/L sodium bicarbonate, all in a 100 mm tissue culture plate. All the culturing mediums had a pH value of 7.2. The normal cell lines, WI38, MARC5, and Beas-2B, were subjected to 7-day cultivation, while the NSCLC cell lines, A549, H1299, and CH27, were subjected to 3-day cultivation in an incubator with 5% CO_2 , at 37°C. All the cell lines were then seeded (2 μL) into the isolation windows located on the PSW sensor surface by micropipette. After 1 h of cultivation in an incubator with 5% CO_2 at 37°C to assure cell adhesion on the γ -APTES surface, the excessive cells adhering outside the γ -APTES region in the isolation window were carefully washed off by dropping phosphate buffer solution (PBS) into isolation window and draining out the overflow PBS solution as well as the excessive cells outside the isolation window with an aspiration pump. We repeated this process several times until all the excessive cells were removed. After the removal of the excessive cells, only a single cell was left in the isolation window for the γ -APTES area is about the size of a single cell. The PSW was then placed into the incubator with 5% CO_2 at 37°C for another 24 h of cultivation. Figure 3(a) shows the top-view images by optical microscopy of the single NSCLC cells A549, H1299, and CH27 as well as the single normal cells Beas-2B, MRC5, and WI38 which were successfully cultivated in the isolation window on the PSW surface, respectively.

2.3 Electrical characterization

After 24 h cell cultivation, the drain-source current I_{DS} flowing through the PSW channel was measured by applying DC biases between the source (S) and drain (D) terminals and using the semiconductor parameter analyzer Agilent 4156C. The current differences with and without a single cell being cultivated inside the isolation window, i.e., $\Delta I = I_{DS}$ (with single cell) - I_{DS} (without single cell), were then obtained. No bias was applied between the side gates. All the electrical measurements were carried out in a light-sealed probe station. Figure 3 (b) shows the schematic diagram of the overall setup for the measurement.

3 Results and discussion

3.1 PSW sensor performance

The linearity and long term stability of the PSW sensor for glucose detection has been reported in our previous work (Hsu et al. 2009) (Wu et al. 2011). In order to confirm the applicability of the PSW sensor for measuring the change in the extracellular microenvironment around a single cell, we again conducted the pH response test for the PBS solution with different pH values. Figure 4(a) shows the amount of channel current change $\Delta I'$ of the PSW compared with the current obtained at a pH value of 7.2. In other words, $\Delta I' = I_{DS} - I_{DS}$ (pH=7.2), measured at the source-drain voltage $V_{DS} = 5$ V as a function of the pH values of the phosphate buffer solution (PBS). It is evident that $\Delta I'$ increases linearly with the pH value of the PBS for pH values ranging from 4 to 10. In addition, in order to avoid possible error reading due to degradation of the sensing membrane caused by long-term immersion in culture medium, we measured the percentage change of the current drifts, i.e. $\{[\Delta I'(t) - \Delta I'(0)] / \Delta I'(0)\} \times 100\%$ measured at $V_{DS} = 5$ V, as a function of time for different cell-free culture mediums, DMEM, BME, MEM and RPMI1640. Each culture medium has a pH value of 7.2, and the results are shown in Fig. 4(b). It is evident that all the culture mediums exhibit only a very small drift (< 2%) during the 40 h of testing. This indicates that long-term immersion in the culture mediums did not lead to degradation of the sensing membrane.

3.2 Single cell characterization

Generally, it takes 1~2 days for a cell to completely adhere to a substrate (Baumann et al. 1999) (Lehmann et al. 2000) (Otto et al. 2003) (Yu et al. 2009). We therefore measured the current changes ΔI of the PSW at $V_{DS} = 5$ V for the single normal cells and the NSCLC cells from the very beginning of seeding the single cell into the isolation window as a function of time. The result is shown in Fig. 5. The first item we noticed in Fig. 5 is that for the first 24 h the ΔI of the PSW increases with time. After that it becomes saturated for both the normal cells and the NSCLC cells. The ΔI saturation indicates that 24 h is needed for a cell to completely adhere to the PSW surface, which is consistent with the data reported in (Baumann et al. 1999) (Lehmann et al. 2000) (Otto et al. 2003) (Cai et al. 2009). The other item we observed from Fig. 5 is that the current change ΔI for all the NSCLC cells is higher than that for the normal cells, indicating that all the NSCLC cells have stronger cell-substrate adhesion than the normal cells. We also noticed that the ordering of the ΔI for the single NSCLC cells is A549 > H1299 > CH27, while for the single

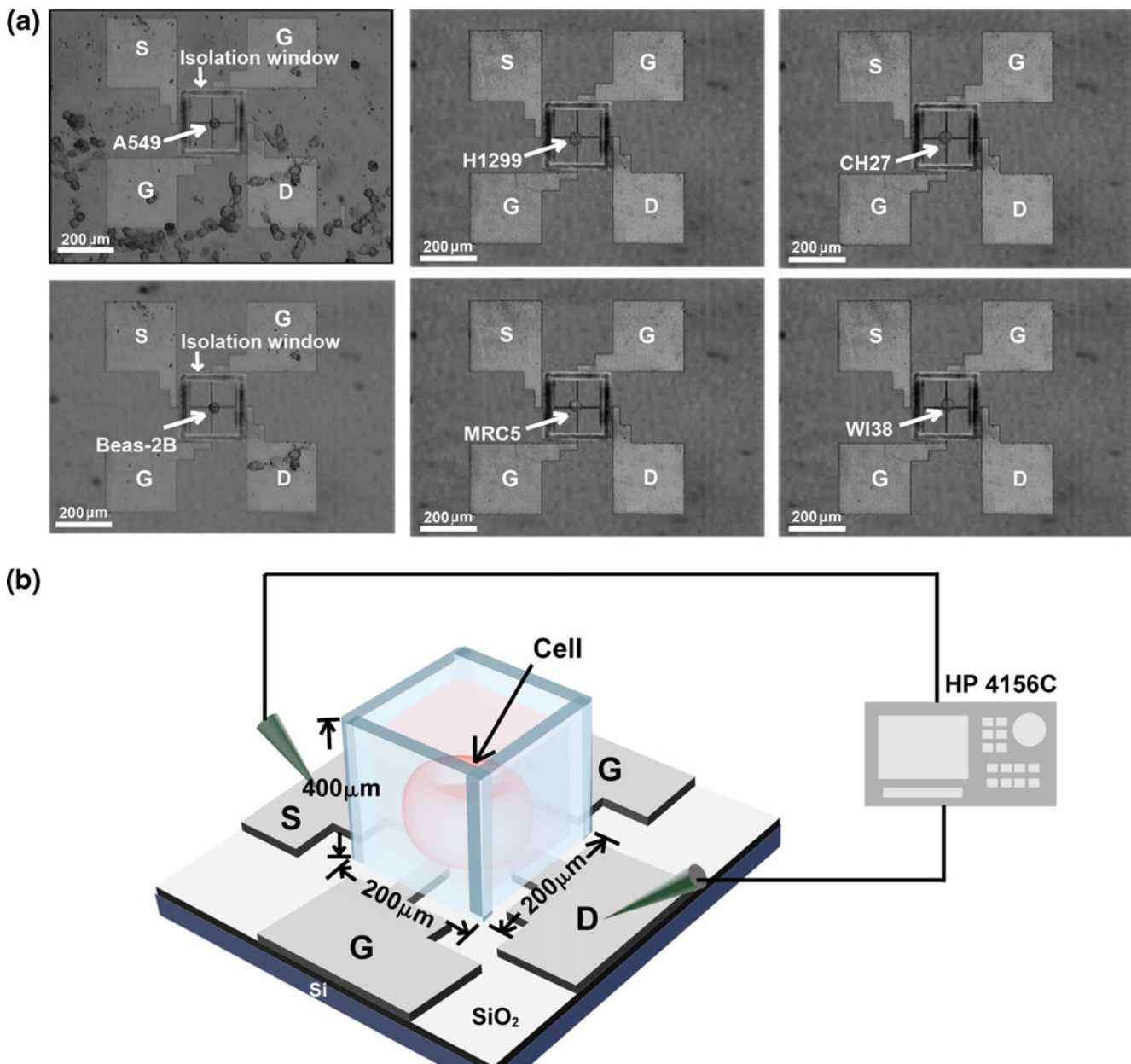


Fig. 3 (a) Top-view pictures by optical microscopy of the PSW sensor integrated with an isolation window inside which single isolated cancer cells A549, H1299, and CH27, as well as a single

isolated normal cells Beas-2B, MRC5 and WI38 were successfully cultured. (b) Schematic diagram of the overall setup for the measurement

normal cells it is Beas-2B>WI38>MRC5, respectively. In other words, the ordering of the ΔI is exactly the same as that of the extracellular pH values of the cells, i.e. 5.86 ± 0.06 for A549, 6 ± 0.08 for H1299, 6.2 ± 0.04 for CH27, and 6.9 ± 0.08 for Beas-2B, 6.96 ± 0.07 for WI38, and 7.02 ± 0.07 for MRC5, respectively. The pH values were determined from the ΔI calibration curve of the PSW sensor for the standard measurement of pH solutions. It has been reported that glucose will be taken up by specific transporters on the cell membrane and then converted, first to glucose-6-phosphate by hexokinase and then to pyruvate,

generating 2 adenosine triphosphate (ATP) per glucose. In this process, H^+ ions are generated, causing acidification of the extracellular microenvironment (Gillies et al. 1994) (McCoy et al. 1995) (Ragunand et al. 1999) (Gatenby and Gillies 2004) (Cardone et al. 2005). Hence, we believe that it is the extracellular acidification of the single cells residing inside the isolation window that causes the PSW current changes. In order to verify this, we first removed the original culture medium and added 1 μL glucose (5 mM) solution (pH=7.2) as a stimulus into the isolation window and tracked the evolution of the pH value (ΔI) changes

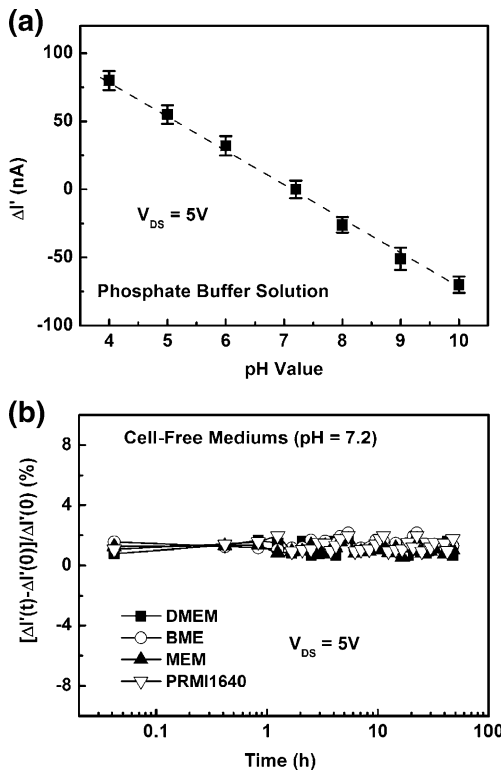


Fig. 4 (a) Channel current changes $\Delta I' = I_{DS} - I_{DS}(pH=7.2)$ of the PSW sensor for the measurement of PBS with different pH values. (b) Percentage changes of the current drifts, $\{[\Delta I'(t) - \Delta I'(0)] / \Delta I'(0)\} \times 100\%$, measured at $V_{DS} = 5V$, as a function of time for different cell-free culture mediums, DMEM, BME, MEM and RPMI1640 dropped by micropipette into the isolation window

over time in the extracellular environment of the single cells. The glucose stimulus was added at 2.5 min after 24 h cultivation of the single cell inside the isolation window, and then the current changes ΔI of the PSWs measured at $V_{DS} = 5V$ as a function of time were recorded as shown in Fig. 6(a). We added the stimulus at 2.5 min after 24 h cultivation to allow enough time to prepare the stimulus solution and make sure that all the stimuli were added at the

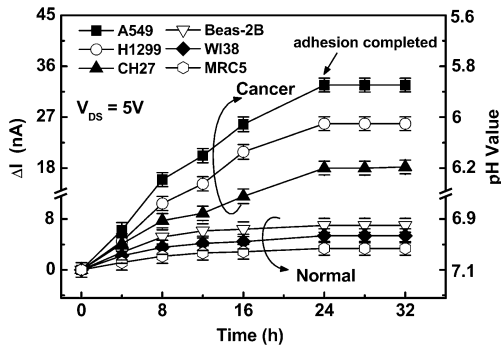


Fig. 5 Channel current changes ΔI of the PSW measured at $V_{DS} = 5V$ for single normal cells and NSCLC cells cultivated from the very beginning of seeding the single cell into the isolation window, as function of time

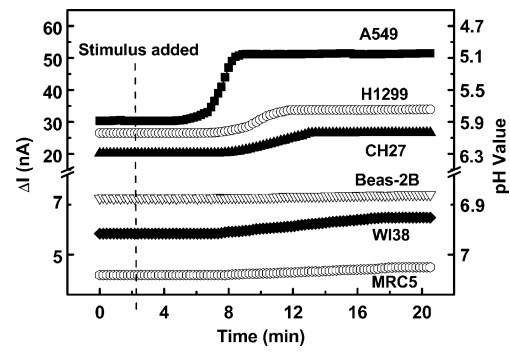


Fig. 6 Current changes ΔI of the PSW sensor measured at $V_{DS} = 5V$ as a function of time, in which a glucose stimulus (pH=7.2) was added at 2.5 min after first removing the original culture medium, for single cells cultivated for 24 h inside the isolation window

same time reference point. It is evident that the ΔI change rate for the normal cells is slower than that for the cancer cells. The ΔI takes about 6–10 min for the NSCLC cells, while it takes about 15 min for the normal cells to become saturated after the glucose stimulus has been added. This result indicates that the NSCLC cells have a higher glucose consumption rate than the normal cells due to upregulation of the glucose transporters (GLUT1 and GLUT3) when the glucose stimulus is added (Gillies et al. 1994) (McCoy et al. 1995) (Raghuhand et al. 1999) (Gatenby and Gillies 2004) (Cardone et al. 2005). From Fig. 6 we can calculate the acidification rate which is 0.102 ± 0.04 , 0.086 ± 0.05 , and 0.06 ± 0.03 pH units/min for the cancer cells A549, H1299 and CH27, respectively, while it is 0.006 ± 0.001 , 0.004 ± 0.001 , and 0.005 ± 0.05 pH units/min for the normal cells Beas-2B, WI38 and MRC5, respectively. It is evident that cancer cells have stronger extracellular acidification than normal cells, and that the extracellular acidification rate of the normal cells is about an order of magnitude lower than that of the NSCLC cells. This is consistent with the results reported in (Gillies and Bhujwala 1994) (McCoy et al. 1995) (Raghuhand et al. 1999) (Gatenby and Gillies 2004) (Cardone et al. 2005).

To ensure that the data shown in Fig. 6 is not a false result due to γ -APTES surface degradation caused by glucose solution, we removed the glucose containing culture mediums in the isolation windows carefully by sucking them out with an aspiration pump along the peripheral of the isolation window and replaced them with fresh glucose-free culture mediums by micropipette, and then again measured the current changes ΔI of the PSW. Figure 7(a) shows the PSW saturation current changes ΔI (i.e. 20 min after adding the glucose stimulus) before and after replacing the glucose-free culture mediums for the cancer cells. Figure 7(b) shows the same but for the normal cells. It is apparent that for both the normal and the cancer cells, all the ΔI 's return to their original values after each

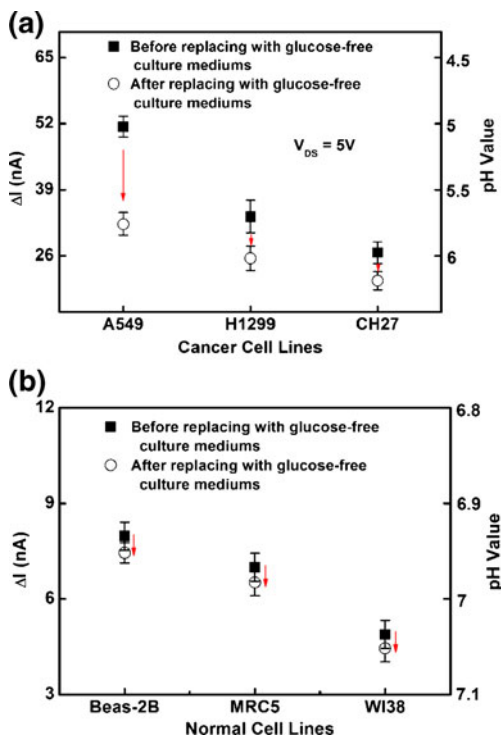


Fig. 7 Saturation current changes ΔI of the PSW sensor after the glucose containing mediums were replaced with fresh glucose-free culturing mediums for single (a) cancer cells and (b) normal cells cultivated inside the isolation window

respective isolation window was refilled with a glucose-free culture medium.

The proposed PSW sensor can also be used to detect the apoptosis of the single cells cultivated on the γ -APTES surface inside the isolation window. Figure 8(a) shows the saturation current changes ΔI 's measured at $V_{DS}=5$ V of the single cancer cells and the normal cells cultivated inside the isolation window as a function of time, where time zero was taken as the time after 24 h cultivation in the incubator with 5% CO_2 at 37°C. In other words, after the cells were completely adhered to the PSW surface. It was observed that, initially, all the ΔI 's remained unchanged for both the NSCLC and the normal cells. However, the ΔI 's for the NSCLC cells began to drop after 4.5 h and became zero after 5.5 h, while those for the normal cells began to drop after 3 h and became zero after 4 h. The ΔI 's drop to zero is believed to be caused by the apoptosis of the cells. Figure 8(b) shows the optical microscopic pictures of the NSCLC cells and the normal cells cultivated inside the isolation window before and after the ΔI 's drop to zero, confirming that the ΔI 's dropping to zero indicates the apoptosis of the cells. It should be noted that the extracellular H^+ ions can only build up on the external surface of the cell membrane (Matsuyama and Reed, 2000), and that they do not dissolve into the culture medium. Therefore, apoptosis of

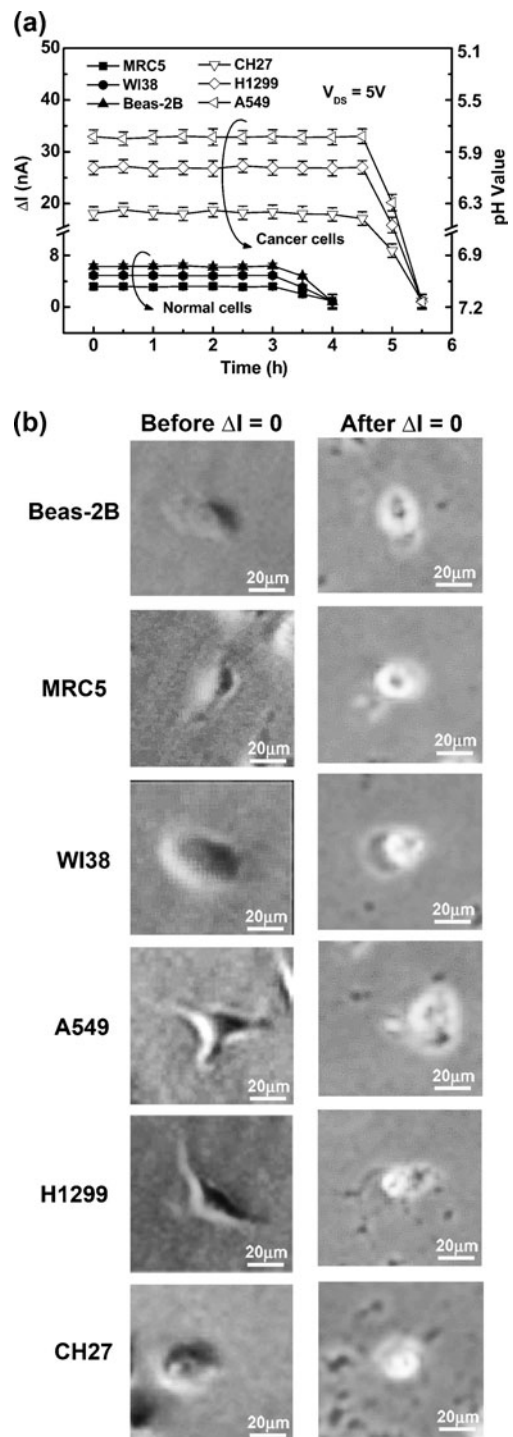


Fig. 8 (a) Saturation current changes (ΔI 's) of the PSW sensor as a function of time measured at $V_{DS}=5$ V of the single cancer cells and normal cells cultivated inside the isolation window, with time zero taken as the time after 24 h cultivation in the incubator with 5% CO_2 at 37°C. (b) Photographs taken by optical microscope of the NSCLC cells and normal cells cultivated inside the isolation window before and after the saturation current changes dropped to zero

the cell does not result in H^+ ions accumulating on the outer surface of the cell membrane, hence a zero PSW

channel current change (Baumann et al. 1999) (Cardone et al. 2005) (Moreno-Sanchez et al. 2007).

The PSW sensor can be reused after an appropriate cleaning procedure. By dropping 1 μ L trypsin into the isolation window and waiting for 1 min in a 5% CO₂, 37°C incubator, and then taking the chip containing the PSW sensor out of the incubator and shaking it very gently until the single cell cultivated inside the isolation window floats over the surface of the culturing medium, the culturing medium and the cell can be drained from the isolation window using an aspiration pump. Alcohol is then dropped into the isolation window and sucked back out. This is repeated two or three times, followed by a final wash with PBS solution, similar to the alcohol cleaning step followed by a drying process in the atmosphere. All these processes are carried out with the help of an optical microscope. The PSW sensor is then sterilized in an autoclave sterilizer and is ready for reuse. For the same PSW sensor, we also conducted 20 successive ΔI 's measurements for each of the normal and each of the NSCLC cells after the cells were completely adhered to the sensor surface, in order to check the stability and reproducibility of the PSW sensor. The relative standard deviations (R.S.D.) were about 4.02%, 4.54% and 4.33% for the normal cells Beas-2B, WI38 and MRC5, respectively, while they were about 4.76%, 4.68% and 4.42%, for the NSCLC cells A549, H1299 and CH27, respectively. The R.S.D. for each cell is less than 5% and assures good stability of the PSW cell biosensor, for both the normal cell and NSCLC sensing. The same cells were also tested on four PSW sensors from four difference fabrication batches. The R.S.D.s for the four tests were 3.42%, 3.38%, 3.57%, for normal cells Beas-2B, WI38 and MRC5, respectively, and 3.45%, 3.82% and 3.57% for NSCLC A549, H1299 and CH27, respectively. It is evident that the use of PSW exhibits excellent reproducibility for the detection of living cells.

4 Conclusions

In this paper, a PSW sensor integrated with a PDMS isolation window was used to detect the microenvironment of an isolated single cell. We used the confinement of a PDMS isolation window inside which a γ -APTES layer with an area similar to the size of a single cell was coated onto the PSW sensor surface. This allowed us to cultivate single normal cells as well as cancer cells inside the isolation window. By observing the changes of the current flowing through the PSW channel, we found that each cell has its own characteristic ΔI , and that NSCLC cells have higher ΔI 's than normal cells. We also determined the evolution of the cell adhesion onto the substrate over time by measuring the ΔI as a function of time. The most

important finding however is that with the PSW sensor we can detect the extracellular acidification of a single cell, and we confirmed that a single cancer cell exhibits higher extracellular acidification and a higher acidification rate than a single normal cell.

Acknowledgement This work was financially supported by the Taichung Veterans General Hospital-National Chi Nan University Joint Research Program under contract no.TCVGH-NCNU977903.

References

- H. Andersson, A. van den Berg, *Curr. Opin. Biotechnol.* **15**, 44–49 (2004)
- W.H. Baumann, M. Lehmann, A. Schwinde, R. Ehret, M. Brischwein, B. Wolf, *Sens. Actuators B Chem.* **55**, 77–89 (1999)
- Y. Berdichevsky, J. Khandurina, A. Guttman, Y.J. Lo, *Sens. Actuators B Chem.* **97**, 402–408 (2004)
- R.A. Cardone, V. Casavola, S.J. Reshkin, *Nat. Rev. Cancer* **5**, 786795 (2005)
- P. Chen, B. Xu, N. Tokranova, X. Feng, J. Castracane, K.D. Gillis, *Anal. Chem.* **75**, 518–524 (2003)
- S. Chen, S.J. Lillard, *Anal. Chem.* **73**, 111–118 (2001)
- H.M. Davey, D.B. Kell, *Microbiol. Rev.* **60**, 641–696 (1996)
- J.E. Ferrell, E.M. Machleder, *Science* **280**, 895–898 (1998)
- K. Fujita, N.I. Smith, *Mol. Cell* **25**, 530–535 (2008)
- D.S. Gray, J.L. Tan, J. Voldman, C.S. Chen, *Biosens. Bioelectron.* **19**, 771–780 (2004)
- R.A. Gatenby, R.J. Gillies, *Nat. Rev. Cancer* **4**, 891–899 (2004)
- R.J. Gillies, Z. Liu, Z. Bhujwalla, *Am. J. Physiol.* **267**, C195–C203 (1994)
- C.Y. Hsiao, C.H. Lin, C.H. Hung, C.J. Su, Y.R. Lo, C.C. Lee, H.C. Lin, F.H. Ko, T.Y. Huang, Y.S. Yang, *Biosens. Bioelectron.* **24**, 1223–1229 (2009)
- P.Y. Hsu, J.J. Lin, Y.L. Wu, W.C. Hung, A.G. Cullis, *Sens. Actuators B Chem.* **142**, 273–279 (2009)
- T.C. Karni, B.P. Timko, L.E. Weiss, C.M. Lieber, *Proc. Natl. Acad. Sci. U.S.A.* **106**, 7309–7313 (2009)
- W. Kern, D.A. Puotinen, *RCA Rev.* **31**, 187–206 (1970)
- S.N. Krylov, N.J. Docichi, *Electrophoresis* **21**, 767–773 (2000)
- M.H. Lee, D.A. Brass, R. Morris, R.J. Composto, P. Ducheyne, *Biomaterials* **26**, 1721–1730 (2005)
- M. Lehmann, W. Baumann, M. Brischwein, R. Ehret, M. Kraus, A. Schwinde, M. Bitzenhofer, I. Freund, B. Wolf, *Biosens. Bioelectron.* **15**, 117–124 (2000)
- S. Matsuyama, J.C. Reed, *Cell Death Differ.* **7**, 1155–1165 (2000)
- C.L. McCoy, C.S. Parkins, D.J. Chaplin, J.R. Griffiths, L.M. Rodrigues, M. Stubbs, *Br. J. Cancer* **72**, 905–911 (1995)
- N.N. Mishra, W.C. Maki, E. Cameron, R. Nelson, P. Winterrowd, S.K. Rastogi, B. Filanoski, G.K. Maki, *Lab Chip* **8**, 868–871 (2008)
- R. Moreno-Sanchez, S. Rodriguez-Enriquez, A. Marin-Hernandez, E. Saavedra, *FEBS J.* **274**, 1393–1418 (2007)
- A.M. Otto, M. Brischwein, A. Niendorf, T. Hanning, E. Motrescu, B. Wolf, *Cancer Detect. Prev.* **27**, 291–296 (2003)
- Patolsky F., Timko B. P., Yu G., Fang Y., Greytak A. Zheng B., G., C. M. Lieber, *Science*, **313** 1100–1104 (2006).
- T.S. Pui, A. Agarwal, F. Ye, N. Balasubramanian, P. Chen, *Small* **5**, 208–212 (2009)
- N. Raghunand, M.I. Altbach, R. van Sluis, B. Baggett, C.W. Taylor, Z. M. Bhujwalla, R.J. Gillies, *Biochem. Pharmacol.* **57**, 309–312 (1999)

- A. Revzin, K. Sekine, A. Sin, R.G. Tompkins, M. Toner, *Lab Chip* **5**, 30–37 (2004)
- M.C. Roco, *Curr. Opin. Biotechnol.* **14**, 337–346 (2003)
- S. Schäfer, S. Eick, B. Hofmann, T. Dufaux, R. Stockmann, G. Wrobel, A. Offenhäusser, S. Ingebrandt, *Biosens. Bioelectron.* **24**, 1201–1208 (2009)
- B. Schnyder, T. Lipperta, R. Kötza, A. Wokauna, Vera-Maria Graubnerb, O. Nuyken, *Surf. Sci.* **532–535**, 1067–1071 (2003)
- C.E. Sims, N.L. Allbritton, *Lab Chip* **7**, 423–440 (2007)
- F. Sommerhage, A. Baumann, G. Wrobel, S. Ingebrandt, A. Offenhäusser, *Biosens. Bioelectron.* **26**, 155–161 (2010)
- M.N. Teruel, T. Meyer, *Science* **295**, 1910–1912 (2002)
- I. Vermes, C. Haanen, C. Reutelingsperger, *J. Immun. Method* **243**, 167–190 (2000)
- L.A. Wood, T.P. Roddy, A.G. Ewing, *Electrophoresis* **25**, 1181–1187 (2004)
- Y.L. Wu, P.Y. Hsu, C.P. Hsu, W.C. Liu, *J. Electrochem. Soc.* **157**, J191–J195 (2010)
- Y.L. Wu, P.Y. Hsu, J.J. Lin, *Biosens. Bioelectron.* **26**, 2281–2286 (2011)
- H. Yu, H. Cai, W. Zhang, L. Xiao, Q. Liu, P. Wang, *Biosens. Bioelectron.* **24**, 1462–1468 (2009)